Observations of antarctic polar stratospheric clouds by the Geoscience Laser Altimeter System (GLAS)

Stephen P. Palm,[1] Michael Fromm,[2] and James Spinhirne[3]

Received 16 May 2005; revised 29 July 2005; accepted 5 August 2005; published 20 September 2005.

[1] We present the first satellite lidar observations of Polar Stratospheric Clouds (PSCs). During late September and early October 2003, GLAS frequently observed type I and II PSCs over western Antarctica. At the peak of this activity on September 29 and 30 we investigate the vertical structure, horizontal coverage and general characteristics of the PSCs using the GLAS data. The PSCs were found to cover a relatively large area in a region where enhanced PSC frequency has been noted by previous PSC climatology studies. We also show near simultaneous measurements from the POAM III and SAGE II satellites that confirm the presence of type I and II PSCs in the same region. The area of PSC formation was found to coincide with the coldest temperatures and highest geopotential height in the lower stratosphere. In addition, extensive cloudiness was seen within the troposphere below the PSCs indicating that tropospheric disturbances played a role in their formation. **Citation:** Palm, S. P., M. Fromm, and J. Spinhirne (2005), Observations of antarctic polar stratospheric clouds by the Geoscience Laser Altimeter System (GLAS), *Geophys. Res. Lett.*, *32*, L22S04, doi:10.1029/2005GL023524.

1. Introduction

[2] The Geoscience Laser Altimeter System (GLAS) was launched aboard the polar-orbiting Ice Cloud and land Elevation Satellite (ICESat) in January 2003 [*Zwally et al.*, 2002]. GLAS utilizes 3 diode-pumped, ND:YAG lasers operating at the fundamental wavelength of 1064 nm for surface altimetry and clouds, and the frequency doubled 532 nm wavelength that provides high sensitivity (photon counting detectors) for atmospheric measurements of thin clouds and aerosols (J. D. Spinhirne et al., Cloud and aerosol measurements from GLAS: Overview and initial results, submitted to *Geophysical Research Letters*, 2005). Both atmospheric channels provide a high resolution (175 m horizontal and 76 m vertical) cross section of clouds and aerosols along the flight track. To date, GLAS has operated in six separate observation periods, each lasting four to six weeks. In total, GLAS has collected over 6 months of data that have provided unique insights into global cloud and aerosol vertical distribution and transport processes.

[3] It is well known that Polar Stratospheric Clouds (PSCs) are frequently observed during the Austral winter over Antarctica. Occurring from late fall to early spring, PSCs have been routinely observed over the last 30 years by limb-sounding instruments such as the Stratospheric Aerosol Measurement (SAM) II, the Stratospheric Aerosol and Gas Measurement (SAGE) I–III and the Polar Ozone and Aerosol Measurement (POAM) II and III [*McCormick et al.*, 1982]. *Fromm et al.* [2003] present a concise climatology of PSC occurrence in both hemispheres covering the period 1979 to 2000 using data from SAM II, SAGE II and POAM II/III. They found that when temperatures in the stratosphere are conducive to PSC formation (i.e. $T < 195$ K), PSCs are detected from the limb measurements 60% of the time for both hemispheres. However, the overall frequency of occurrence of PSCs is some 5–10 times greater in the Antarctic because of the stability of the polar vortex and the lower temperatures found there. More recently, limb sounding infrared spectrometers have been used to detect the presence of PSCs from their emission spectra. The Cryogenic Spectrometers and Telescopes for the Atmosphere (CRISTA) instrument examined Antarctic PSCs and measured distinctive spectral features that are attributed to the NO_3 ion, strongly suggesting a condensed nitric acid component to the particles in the form of solid nitric acid trihydrate (NAT) [*Spang and Remedios*, 2003]. The Michelson Interferometer for Passive Atmospheric Sounding (MIPAS) was used to map the frequency and geographic occurrence of PSCs during the Artic winter of 2002–2003 [*Spang et al.*, 2005].

[4] The ubiquity of PSCs makes them ideal targets for observation by a polar orbiting lidar such as GLAS. The second ICESat observation period (Laser 2a; September 25–November 18, 2003) covered the latter part of the Antarctic PSC season and provided the first ever opportunity to sample PSCs from a satellite lidar. During the first week of this period, type II water ice PSCs were evident in the GLAS data over a fairly large area of Antarctica. The PSC frequency and coverage peaked on September 30, but a significant amount of type I PSCs were seen to occur through October 13th. After this date, and until the end of operations (November 18), GLAS did not observe PSC formation. In this paper we will focus on GLAS, SAGE II and POAM III PSC observations from September 29 and 30, 2003.

2. Glas Observations

[5] On the September 29 and 30 2003, GLAS detected a large area of enhanced attenuated backscatter (GLA07) reaching to heights of 21 km, and often extending down to the ground. During this 48-hour period, a total of 16 (of a possible 30) ICESat tracks were found to contain PSCs (track numbers from cycle 29: 22, 23, 30, 31, 32, 33, 34, 36, 37, 38, 42, 43, 44, 45, 46 and 47). The locations of all 30 ICESat tracks for this two-day period are shown as the

[1]Science Systems and Applications Inc., Lanham, Maryland, USA.
[2]Naval Research Laboratory, Washington, DC, USA.
[3]Goddard Space Flight Center, Greenbelt, Maryland, USA.

0094-8276/05/2005GL023524$05.00

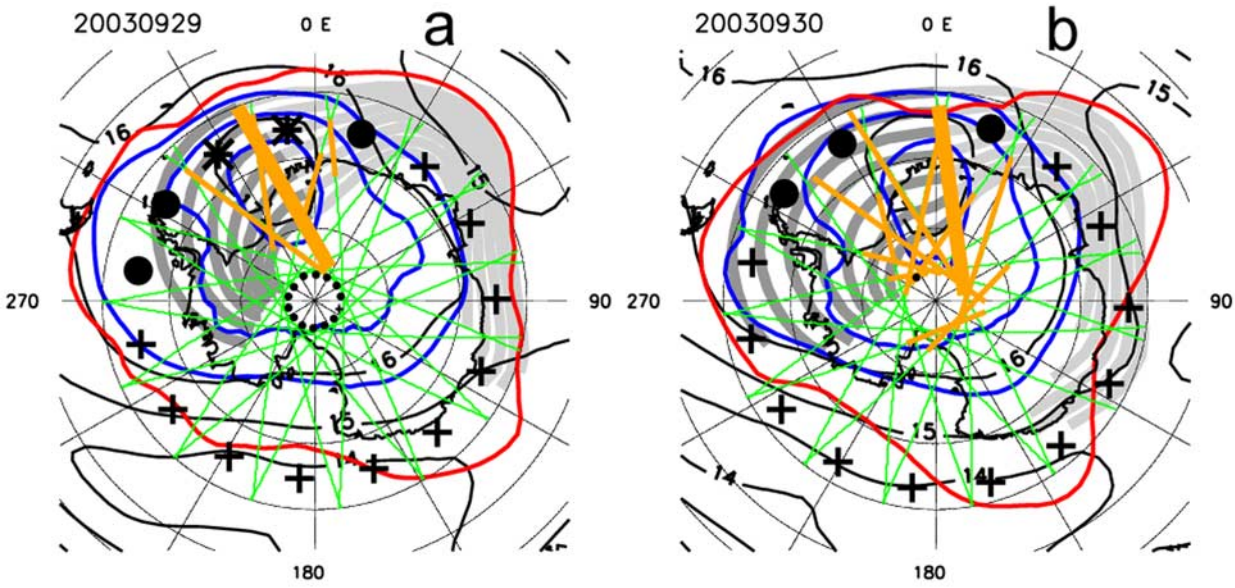

Figure 1. Map of Antarctica showing the ICESat tracks (green), GLAS observed PSC locations (orange), geopotential height (km) of the 400 K potential temperature surface (black contours), PSC locations from POAM III (small black dots), and SAGE II (large black dots and asterisks) for September (a) 29 and (b) 30, 2003. Temperature contours at 185K (innermost contour), 190K, and 195K are shown in blue. Also shown are the 4-day back trajectories (thick, dark gray lines) and forward trajectories (thick, light gray lines) for parcels at 18 km altitude originating along the GLAS tracks shown in Figure 2. The plus symbols represent SAGE II measurements that did not detect PSC. The red line marks the position of the edge of the polar vortex.

green lines in Figure 1. The orange segments of those tracks represent the areas where PSCs were observed. Examples of the GLAS-measured 532 nm backscatter ratio (total scattering divided by the molecular or Rayleigh scattering) for September 29 and 30 are shown in Figure 2. This figure shows two very large PSCs stretching roughly 3000 km from over the central portion of Antarctica, the Weddell Sea and ending near latitude 62°S. The very tenuous top portion of the cloud with backscatter ratios between 2 and 5 in Figure 2a (September 29) extends to a height of 21 km and is the highest PSC top observed by GLAS during this period. Based on the magnitude of the backscatter ratio and the fact that the temperature at 18–20 km is about 192K (from ECMWF temperature analysis), it is likely that this portion of the cloud (between 18–21 km) is a type I PSC. Other lidar investigations have categorized PSCs based on backscatter and depolarization ratio [*Browell et al.*, 1990; *Adriani et al.*, 2004]. Type I PSCs typically have backscatter ratios less than 10 and exhibit a depolarization less than 35–40%. Type II PSCs display much larger backscatter ratios with peak values ranging from 20–100, and larger depolarization. GLAS cannot measure the depolarization and thus must rely on the backscatter ratio and temperature to differentiate between type I and II. Also of note in Figure 2a is the slightly enhanced scattering region between 12 and 16 km altitude at the extreme left portion of the image (86°S–83°S). This is near the location of a POAM III retrieval indicating the presence of a PSC (small black dots in Figure 1a). The magnitude of this enhanced area of scattering is so small, it is just barely discernable in the GLAS data and is most likely a type I PSC. This shows that the scattering from some type I PSCs is very close to the detection limit for the GLAS 532 nm channel. Below 18 km to the tropopause, atmospheric temperatures are low enough to support type II water ice PSCs (ECMWF analysis show a temperature minimum at 13 km of 182K). The 532 nm backscatter ratios are as high as 40 throughout the cloud at altitudes of 17–18 km. Lower in the cloud (8–12 km), backscatter ratios exceed 50 but this portion of the cloud resides within the troposphere. A temperature sounding from September 29 taken at 70.9S, 8W indicated a tropopause height of about 13 km (based on the standard WMO definition). Also shown in Figure 2 is the tropopause height (yellow line) along the GLAS track computed from the UKMO meteorological analyses [*Swinbank and O'Neill*, 1994] based on potential vorticity (i.e. the height of the pv = 3 10^{-6}m^{2}Ks^{-1}kg^{-1} surface). The maximum tropopause height (13.2 km) occurs at 72.5S, which is very close to the deepest part of the PSC shown in Figure 2a. Also, note how the arching of the cirrus shield in Figure 2a closely follows the tropopause height, especially in the right half of the figure.

[6] Figure 2b shows the 532 nm backscatter ratio from a track on September 30th that is located to the east of the track shown in Figure 2a. The location of this track is shown as the thick orange line in Figure 1b. The PSC is similar in character and appearance to the PSC from the day before (Figure 2a). This cloud extends to 20 km and covers a distance of about 2800 km. Like the PSC in Figure 2a, there appears to be a separation or discontinuity at about 12 km altitude, which is in fact the location of the tropopause. A temperature sounding taken at 71S, 8W indicated a tropopause at 11.5 km and the dynamical tropopause height, shown as the yellow line on the image,

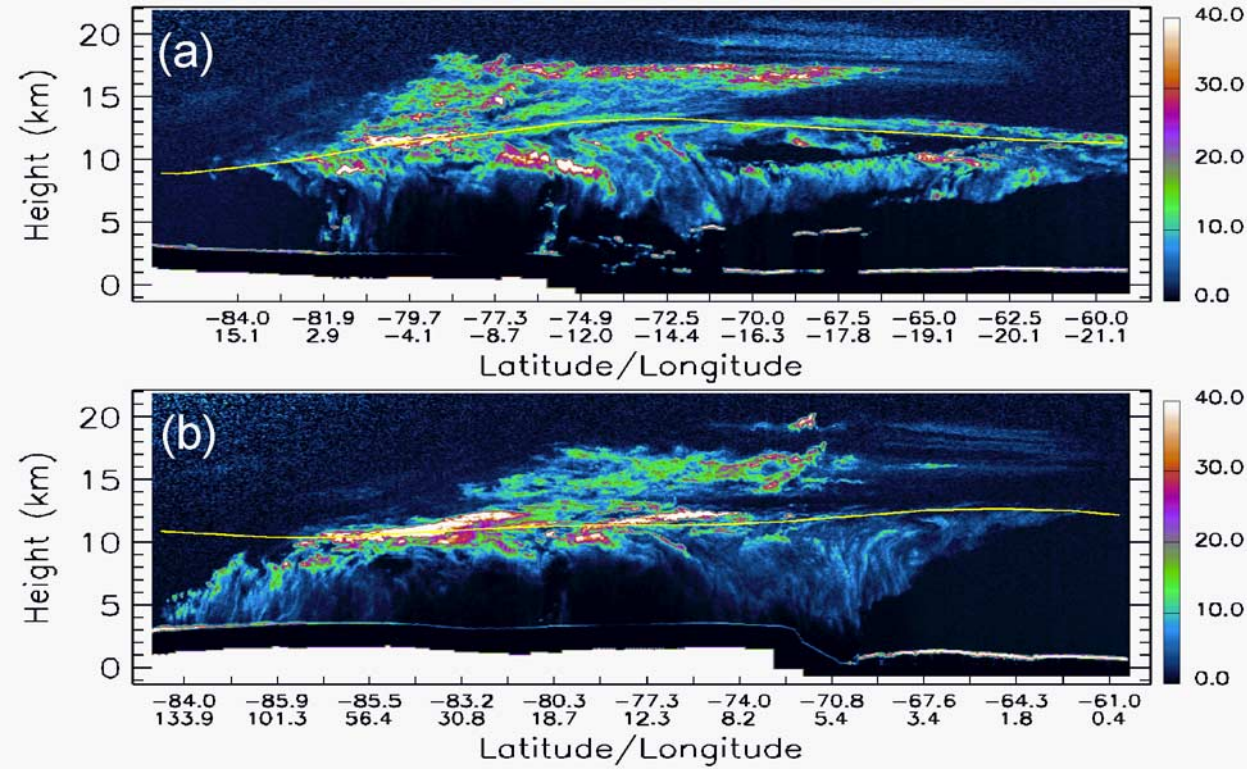

Figure 2. GLAS-measured 532 nm attenuated backscatter ratio (total scattering/molecular) for September (a) 29 and (b) 30, 2003. Highest backscatter ratios exceed 50 (white) between 8 and 12 km. The total length of the PSCs is roughly 3000 km. These tracks correspond to the thicker of the orange lines in Figure 1. The yellow line is the height of the tropopause as described in the text.

agrees well with this value. The 532 nm backscatter ratio reaches a maximum of 62 at about this level. A very thin type I PSC can be seen in Figure 2a at roughly 85S, 55E at an altitude of 15 km. The 532 nm backscatter coefficient values within this PSC are typically about 2.0×10^{-7} $m^{-1}sr^{-1}$. *Reichardt et al.* [2002] performed model calculations on the scattering characteristics of NAT crystals and found that the 532 nm extinction to backscatter ratio for crystals greater than about 1.2 μm is between 10 and 20. If we use an extinction to backscatter ratio of 10 for type I PSCs, we obtain an extinction value of 2.0×10^{-3} km^{-1} for the GLAS type I PSC measurements. This is very consistent with the POAM III extinction retrieval for this day at 86S, 38.1W (1.0×10^{-3} km^{-1}).

3. Discussion

[7] *Teitelbaum et al.* [2001] argued that a major formation mechanism of Arctic PSCs is synoptic scale tropospheric disturbances. They concluded that anticyclonic potential vorticity anomalies near the tropopause induce an upward displacement of the isentropic surfaces in the lower stratosphere. This causes synoptic scale quasi-adiabatic lifting and cooling of the air resulting in the PSC formation or thickening. *Tuck* [1989] made a similar argument for Antarctic PSCs observed in Austral winter of 1987. If this is the causative mechanism for the PSCs seen by GLAS, it follows that they would have dimensions on the order of 1000 km since this is a characteristic dimension of synoptic scale disturbances. Additionally, there is extensive cloudiness within the troposphere below both PSCs, indicating a likelihood that a tropospheric disturbance is playing a role in the PSC formation. It is possible that all the PSCs detected by GLAS over this two day period may be different portions of a single very large PSC that has persisted for at least 2 days and possibly much longer.

[8] In addition to the ICESat tracks, Figure 1 gives the UKMO geopotential height (black contour lines) of the 400 K potential temperature surface (roughly 15 km altitude), the location of the polar vortex (red) and the 185°K, 190K, and 195K (blue) temperature contours for September 29 and 30. Note the location of the geopotential height maximum with respect to the GLAS PSC observations. The deepest PSC activity is seen to occur over the ridge, where the isentropic surfaces have been uplifted with respect to the surroundings. The geopotential height pattern is a manifestation of synoptic scale planetary waves. The winds at this level are westerly and the 4-day back trajectories (thick dark gray lines) and forward trajectories (thick light gray lines) are shown in Figure 1. The winds are moving faster than the planetary waves and the air parcels are subject to vertical motions induced by the tilt of the isentropic surfaces. Namely, over the ridge, the air is rising and cooling, causing saturation and formation of PSCs. Further east, the air is sinking and warming and PSC formation is suppressed. Note that the ridge propagates eastward with time as does the location of the deepest PSC as seen by GLAS.

[9] Also shown in Figure 1 are the locations of PSCs that were detected by POAM III (small black dots) and

SAGE II (large black dots and asterisks). On September 29, SAGE II detected two ice PSCs (asterisks) straddling the region of deepest PSCs seen by GLAS. That these are ice PSCs is inferred from the anomalously high SAGE II profile-termination altitude, a phenomenon *Fromm et al.* [2003] call a High Zmin. POAM III measurements were confined to the 86° latitude circle around which type I PSCs were observed at nearly all longitudes. On September 30, GLAS found type II PSCs over a larger areal extent but only type I PSCs were detected by SAGE and POAM. Note that on the 30th, POAM made only one observation, but that on October 1st, POAM observed PSCs at all 15 measurement locations. The SAGE/POAM, and GLAS PSC observations show how the true ice-PSC coverage is much smaller than the nominal ice pool. That strongly indicates dehydration, which we know has already occurred, since it is late in the PSC season. An interesting further observation to be made is the location of the PSCs observed by GLAS. The analysis performed by *Fromm et al.* [1997] on the distribution and frequency of Antarctic PSCs for the years 1994–1996 revealed that PSCs preferentially form in a certain region of Antarctica. For that time period, the maximum frequency of occurrence of PSCs lies between 315°E and 0°E. The center of PSC activity observed by GLAS is directly in the middle of this area, which lies generally downstream of the Antarctic Peninsula. It is well known that gravity waves frequently occur in this region and are associated with PSC formation [*Wu and Jiang*, 2002]. While it is possible that gravity waves are playing a role in the formation of the observed PSCs, it is likely that synoptic-scale tropospheric disturbances are also impacting stratospheric temperatures and thus PSC development.

4. Conclusions

[10] We have presented the first satellite lidar observations of Antarctic PSCs. The observations shown here are from the last two days of September 2003, and clearly demonstrate the vast size of these clouds. Reaching at times from the tropopause to 21 km, PSCs as long as 3500 km in the horizontal were observed in the 532 nm backscatter channel of GLAS. Of the 30 total ICESat tracks acquired over Antarctica during this time, 16 of them contained PSCs. This, together with the spatial pattern of the PSC observations, leads us to believe that over these two days, GLAS was sampling different portions of a single large PSC or cluster of PSCs. The backscatter ratio of the clouds varied significantly with height, with low values (2–5) above 18 km, moderate values (10–30) between 12 and 18 km, and extremely large values (>60) in the region 8–12 km. Based on meteorological data (not shown), the tropopause is around 12–13 km in the region of deepest PSC formation and temperatures between 13 and 18 km were cold enough (<185°K) to support water ice (type II) PSCs. Outside of this cold region, type I PSCs were observed on both days and were seen to be very close to the detection limit for GLAS. The PSCs were observed over a large area of Antarctica and the Weddell Sea between roughly 280°E and 0°E, congruent with the coldest stratospheric temperatures and highest geopotential height. Prior work has shown that this is a region displaying a climatological maximum of PSC occurrence. Other work [*Tuck* 1989; *Teitelbaum et al.*, 2001] has shown a relationship between tropospheric synoptic scale disturbances and PSCs. While this aspect could not be fully explored here, GLAS does observe a substantial amount of tropospheric cloudiness below the PSCs indicating the presence of a tropospheric disturbance. This remains a topic worthy of future research in which GLAS and future satellite lidars will undoubtedly play a significant role.

[11] **Acknowledgment.** We thank NASA's ICESat Science Project and the NSIDC for distribution of the ICESat data, see http://icesat.gsfc.nasa.gov and http://nsidc.org/data/icesat.

References

Adriani, A., P. Massoli, G. Di Donfrancesco, F. Cairo, M. L. Moriconi, and M. Snel (2004), Climatology of polar stratospheric clouds based on lidar observations from 1993 to 2001 over McMurdo Station, Antarctica, *J. Geophys. Res.*, *109*, D24211, doi:10.1029/2004JD004800.

Browell, E. V., S. Ismail, A. F. Carter, N. S. Higdon, C. F. Butler, P. A. Robinette, O. B. Toon, M. R. Schoeberl, and A. F. Tuck (1990), Airborne lidar observations in the wintertime Arctic Stratosphere: Polar stratosphere clouds, *Geophys. Res. Lett.*, *17*, 385–388.

Fromm, M. D., J. D. Lumpe, R. M. Bevilacqua, E. P. Shettle, J. Hornstein, S. T. Massie, and K. H. Fricke (1997), Observations of Antarctic polar stratospheric clouds by POAM II: 1994–1996, *J. Geophys. Res.*, *102*, 23,659–23,672.

Fromm, M., J. Alfred, and M. Pitts (2003), A unified, long-term, high-latitude stratospheric aerosol and cloud database using SAM II, SAGE II, and POAM II/III data: Algorithm description, database definition, and climatology, *J. Geophys. Res.*, *108*(D12), 4366, doi:10.1029/2002JD002772.

McCormick, M. P., H. M. Steele, P. Hamill, W. P. Chu, and T. J. Swissler (1982), Polar stratospheric cloud sightings by SAM II, *J. Atmos. Sci.*, *39*, 1387–1397.

Reichardt, J., S. Reichardt, P. Yang, and T. J. McGee (2002), Retrieval of polar stratospheric cloud microphysical properties from lidar measurements: Dependence on particle shape assumptions, *J. Geophys. Res.*, *107*(D20), 8282, doi:10.1029/2001JD001021.

Spang, R., and J. Remedios (2003), Observations of a distinct infra-red spectral feature in the atmospheric spectra of polar stratospheric clouds measured by the CRISTA instrument, *Geophys. Res. Lett.*, *30*(16), 1875, doi:10.1029/2003GL017231.

Spang, R., J. Remedios, L. J. Kramer, L. R. Poole, M. D. Fromm, M. Muller, G. Baumgarten, and P. Konopka (2005), Polar stratospheric cloud observations by MIPAS on ENVISAT: Detection method, validation and analysis of the Northern Hemisphere winter 2002/2003, *Atmos. Chem. Phys.*, *5*, 679–692.

Swinbank, R., and A. O'Neill (1994), A stratosphere-troposphere data assimilation system, *Mon. Weather Rev.*, *122*, 686–702.

Teitelbaum, H., M. Moustaoui, and M. Fromm (2001), Exploring polar stratospheric cloud and ozone minihole formation: The primary importance of synoptic-scale flow perturbations, *J. Geophys. Res.*, *106*, 28,173–28,188.

Tuck, A. F. (1989), Synoptic and chemical evolution of the Antarctic vortex in late winter and early spring, 1987, *J. Geophys. Res.*, *94*, 11,687–11,737.

Wu, D. L., and J. H. Jiang (2002), MLS observation of atmospheric gravity waves over Antarctica, *J. Geophys. Res.*, *107*(D24), 4773, doi:10.1029/2002JD002390.

Zwally, H. J., et al. (2002), ICESat's laser measurements of polar ice, atmosphere, ocean, and land, *J. Geodyn.*, *34*, 405–445.

M. Fromm, Naval Research Laboratory, 4555 Overlook Ave., SW, Washington, DC 20375, USA. (mike.fromm@nrl.navy.mil)

S. P. Palm, Science Systems and Applications Inc., 10210 Greenbelt Road, Suite 600, Lanham, MD 20706, USA. (spp@virl.gsfc.nasa.gov)

J. Spinhirne, Goddard Space Flight Center, Greenbelt, MD 20771, USA. (jspin@virl.gsfc.nasa.gov)